Evidence for the Role of the *monB* Genes in Polyether Ring Formation during Monensin Biosynthesis

Andrew R. Gallimore,[1] Christian B.W. Stark,[1,3]
Apoorva Bhatt,[2,4] Barbara M. Harvey,[2]
Yuliya Demydchuk,[2] Victor Bolanos-Garcia,[2]
Daniel J. Fowler,[1] James Staunton,[1] Peter F. Leadlay,[2]
and Jonathan B. Spencer[1,*]
[1] Department of Chemistry
[2] Department of Biochemistry
University of Cambridge
Cambridge, CB2 1EW
United Kingdom

Summary

Ionophoric polyethers are produced by the exquisitely stereoselective oxidative cyclization of a linear polyketide, probably via a triepoxide intermediate. We report here that deletion of either or both of the *monBI* and *monBII* genes from the monensin biosynthetic gene cluster gave strains that produced, in place of monensins A and B, a mixture of C-3-demethylmonensins and a number of minor components, including C-9-*epi*-monensin A. All the minor components were efficiently converted into monensins by subsequent acid treatment. These data strongly suggest that epoxide ring opening and concomitant polyether ring formation are catalyzed by the MonB enzymes, rather than by the enzyme MonCII as previously thought. Consistent with this, homology modeling shows that the structure of MonB-type enzymes closely resembles the recently determined structure of limonene-1,2-epoxide hydrolase from *Rhodococcus erythropolis*.

Introduction

Cyclic polyethers represent an important and extensive family of polyketide natural products. These include a large number of polyether antibiotics [1], as well as highly elaborate marine toxins, such as brevetoxin [2] and maitotoxin [3]. Monensins A and B are typical polyether antibiotics, acting as specific ionophores to dissipate ionic gradients across cell membranes [4]. As early as 1974, Westley proposed that the polyether tetrahydrofuran and tetrahydropyran rings were formed by the sequential opening of a polyepoxide precursor [5]. On the basis of later experiments with labeled precursors, the biosynthesis of monensins was accordingly proposed to involve the intermediacy of a linear *E*-, *E*-, *E*-polyketide triene [6], which is stereospecifically epoxidized to a triepoxide. The triepoxide then undergoes a cascade of S_N2 epoxide openings to give a unique polyether product (Figure 1). An alternative mechanistic

proposal, based on chemical precedent, invoked iron oxetane intermediates, starting from a *Z*-, *Z*-, *Z*-triene [7]. More recently, information from the sequencing of the monensin [8, 9] and nanchangmycin [10] biosynthetic gene clusters has given support to the main outlines of the triepoxide hypothesis. Each cluster contains genes encoding a non-haem, flavin-dependent monooxygenase (*monCI* and *nanO*) and an enzyme displaying homology to authentic epoxide hydrolases (*monCII* and *nanE*) that could function as the key epoxide-opening cyclase enzyme [8–10]. Two novel genes (*monBI* and *monBII*), whose products show significant sequence similarity to known Δ^5-3-ketosteroid isomerases [11], were also found in the monensin cluster. This prompted the suggestion [8, 9] that the products of these genes might isomerize two trisubstituted double bonds on the growing polyketide chain in order to produce a *Z*-, *Z*-, *E*-triene intermediate that could also undergo stereospecific epoxidation and ring opening to monensin. The counterpart in nanchangmycin biosynthesis is the internally duplicated *nanI* gene that appears to comprise *monBI* and *monBII* homologs fused head to tail [10]. This suggested role for MonB and NanI proteins has however been undermined by our recent finding that a mutant of the monensin-producing strain of *Streptomyces cinnamonensis*, in which *monCI* has been deleted, accumulates a triene shunt metabolite that has the *E*-, *E*-, *E*- configuration exclusively [12]. Meanwhile, other recent work in our laboratory has shown that the enzyme originally thought to function as the key epoxide hydrolase/cyclase (MonCII) is likely to be involved in polyketide chain release [13]. This has prompted us to reexamine the role of the MonB proteins, and especially their possible function as epoxide hydrolases/cyclases.

Results and Discussion

MonBI as a Putative Epoxide Hydrolase and Member of the Adaptable α + β Barrel Fold Superfamily
Comparison of the MonB and NanI proteins to proteins in the PDB database by using the program FUGUE [14] readily identified their striking similarity to an emerging family of proteins sharing the same fold but having diverse catalytic or binding activities. The archetype of this family is scytalone dehydratase, which catalyzes key steps in the fungal synthesis of melanin, involving α-proton abstraction, leading to elimination of water and aromatization [15]. Other prominent members include the following enzymes whose crystal structures have also been determined to high resolution: limonene-1,2-epoxide hydrolase from *Rhodococcus erythropolis* (PDB entry 1NWW, 1.2 Å) [16]; the polyketide cyclase SnoaL from *Streptomyces nogalater* (PDB entry 1SJW, 1.3 Å), which catalyzes intramolecular aldol condensation in the closure of the A ring of the anthracycline antibiotic nogalamycin [17]; and Δ^5-3-ketosteroid isomerase from *Pseudomonas putida* (PDB entry 1OPY, 1.9 Å) [18]. Analysis of the superimposed 3D structures of 1NWW, 1SJW, and 1OPY with DALI (http://www.ebi.ac.uk/dali/) [19] reveals a highly conserved fold, with

*Correspondence: jbs20@cam.ac.uk
[3] Present address: Freie Universität Berlin, Institut für Chemie-Organische Chemie, Takustrasse 3, 14195 Berlin, Germany.
[4] Present address: Howard Hughes Medical Institute, Albert Einstein College of Medicine, Department of Microbiology and Immunology, Bronx, New York 10461.
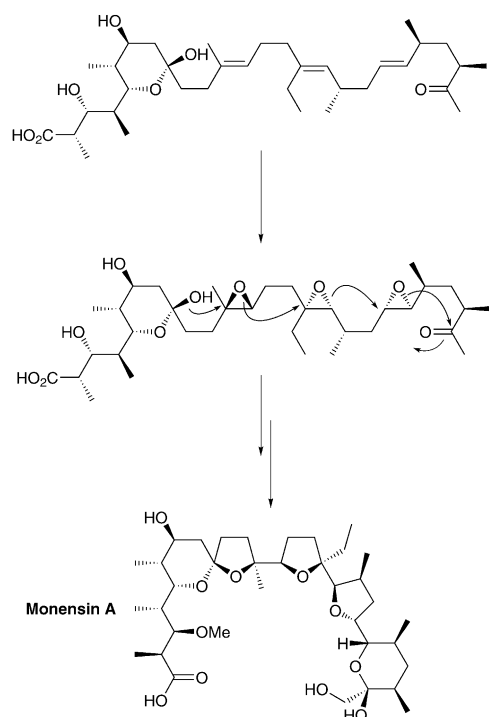
Figure 1. Proposed Mechanism for Monensin Biosynthesis Involving Stereospecific Ring Opening of a Triepoxide Formed from an *E*-, *E*-, *E*-Triene Precursor

the maximum rms deviation ranging between 2.4 Å (between 1OPY and 1SJW) and 2.0 Å (between 1NWW and 1OPY). The closest structural template for MonBI and MonBII is the limonene epoxide hydrolase from *R*. *erythropolis* [16], and the alignment of its sequence with those of the MonB and NanI proteins clearly shows the high conservation of secondary structural elements (Figure 2A). The 3D model generated for MonBI corresponds to a single domain that has been dubbed the adaptable α + β barrel fold [20]. The close superimposition of the modeled structure on the template is shown in Figure 2B. The α + β barrel fold comprises a curved, six-stranded mixed β sheet, with four α helices packed onto it to create a barrel-like structure housing a conical pocket open at its larger end. Most residues lining this pocket are hydrophobic, as in the other proteins of this family. In all other proteins of the family, the pocket contains the active site, and a number of polar amino acid residues are present here and play a role in catalysis. For example, as shown in Figure 2C, the active site of limonene epoxide hydrolase contains two aspartate residues, one (D101) acting as a general acid to promote opening of the epoxide ring, and the other (D132) acting as a general base to assist the nucleophilic attack of a water molecule. A tyrosine residue (Y53) is also proposed to participate as a general base. Likewise, for the ketosteroid isomerases [11, 18], a conserved aspartic acid (corresponding to D37 in MonBI; Figure 2A) is the key general base that abstracts the proton from the substrate. The MonB and NanI proteins do not share conserved active site residues with any of the previously studied proteins of this superfamily. However, between MonBI, MonBII, and the domains NanIa and NanIb, there

are a number of wholly conserved polar residues, including ones (for example, E36 and E64) that are predicted to lie deep within the hydrophobic pocket (Figure 3B) and that are plausible candidates as active site residues involved in acid-base catalysis. Although such ideas require experimental testing, this detailed analysis serves to confirm that the inferred structure of the MonB and NanI proteins is compatible with the proposal made here: that they function as epoxide hydrolases akin to limonene epoxide hydrolase.

Small-Angle X-Ray Scattering Confirms a Dimeric Structure for MonBI

The quaternary structure of the members of the adaptable α + β barrel fold family is highly variable, ranging from dimeric (limonene epoxide hydrolase [16], Δ^5-3-ketosteroid isomerase [18]) to trimeric (scytalone dehydratase [15]), tetrameric (SnoaL [17]), and even tetradecameric (α subunit of calmodulin-dependent kinase II [21]). The MonBI protein was initially modeled as a homodimer based on its similarity with limonene epoxide hydrolase (1NWW). The two monomers of the symmetrical dimer pack against each other via hydrophobic and electrostatic interactions that involve the side chains of residues on the "back face" of the β sheet. A similar dimeric interface has been observed in the crystal structures of 3-oxo-Δ^5-steroid isomerase (1OPY) and limonene epoxide hydrolase (1NWW). It is also found in the polyketide cyclase SnoaL (1SJW), which is organized as a dimer of dimers.

Expression and purification of histidine-tagged MonBI protein from recombinant *Escherichia coli* (see Experimental Procedures) allowed direct estimation of its molecular mass and analysis of its quaternary structure. As judged by gel filtration (data not shown), the protein appeared dimeric. Small-angle X-ray scattering (SAXS) was then carried out on MonBI in solution to confirm its oligomeric structure and to probe its overall size and shape [22]. Shape reconstruction from these data showed an excellent fit of the experimentally determined electron density envelope of the protein to that predicted on the basis of the homology model (Figure 3A and Supplemental Data available with this article online).

Deletion of the *monB* Genes

In-frame deletion mutants deficient in one or both of the *monB* genes of *S*. *cinnamonensis* were produced as described previously [9]. Each of the mutants (AB∆*BI* and AB∆*BII* and the double mutant AB∆*BIBII*) was fermented in monensin production medium, and extracts were analyzed by LC-MS and compared to those from wild-type *S*. *cinnamonensis*. The LC-MS profiles of the mutants appeared to be identical in each case and very different from wild-type (Supplemental Data). No trace of either monensin A (retention time of 17 min) or monensin B (retention time of 15 min) was found, confirming that the *monB* genes are essential for monensin production [9], but also extending that analysis to show the presence, as major products of all three mutants, of the C3-demethyl analogs of monensin A and B, at about 5% of the levels of monensins normally seen in wild-type extracts. Numerous minor components were also present, eluting with retention times between 3 and 10 min under these conditions (see Supplemental Data).

Figure 2. Homology of MonBI and MonBII to Limonene Epoxide Hydrolase

(A) Amino acid sequence alignment of MonBI and MonBII from *Streptomyces cinnamonensis* [8, 9], Nan1A and Nan1B (the N- and C-terminal halves of NanI, respectively) from *Streptomyces nanchangensis* [10], and limonene-1,2-epoxide hydrolase from *Rhodococcus erythropolis* (LEH) (PDB entry 1NWW) [16]. Secondary structural elements of LEH are shown in EScript format (http://escript.ibcp.fr/EScript/cgi-bin/EScript.cgi).

(B) Superposition of the modeled structure of MonBI and the crystal structure of LEH (INWW). For clarity, only one protomer each of MonB1 and of LEH is shown, although both proteins are dimers in solution (see the text).

(C) Proposed reaction mechanism of the LEH-catalyzed reaction (redrawn from [16]).

Isolation and Characterization of *epi*-Monensin A

In order to facilitate the isolation of minor metabolites, the *monBII* gene was deleted in a monensin-overproducing industrial strain of *S. cinnamonensis* exactly as for wild-type. From the fermentation extracts of this strain, a metabolite was obtained with the same accurate molecular mass as monensin A, but with a retention time of 16 min (i.e., about 1 min earlier than monensin A). NMR analysis, including ¹H-NMR NOESY data (Supplemental Data), suggested that this monensin isomer is the C-9-epimer, *epi*-monensin A. This metabolite, which

is not present in wild-type *S. cinnamonensis* cultures, differs from monensin A only in the stereochemistry of the spiroketal center. The fragmentation of the metabolite in electrospray MSMS also differed characteristically from that of monensin A [23].

Spiroketals epimerize under acidic conditions to the more thermodynamically favored configuration [24]. We thus predicted that our putative C-9-epimer should revert to authentic monensin A and confirm our interpretation of the NMR data. Treatment of *epi*-monensin A with HF [25] did indeed result in complete conversion

Figure 3. Model of MonBI Highlighting Residues that May Be Important for Catalysis

(A) Shape reconstruction of dimeric MonBI. The experimental electron envelope for this protein, derived from measurement of small-angle X-ray scattering in solution (SAXS) (see Supplemental Data), together with the 3D structure of MonBI generated by comparative modeling, is displayed by using the program PyMol [41]. In each protomer, two conserved, buried polar residues potentially involved in catalysis, E36 and E64, are highlighted in red.

(B) Electrostatic surface representation of a MonBI protomer showing the location of E36 and E64 inside the hydrophobic cavity.

to monensin A. Subsequently, a much more abundant novel metabolite, the C-26-deoxy analog of *epi*-monensin A, was also isolated from the fermentation extracts of the mutant and eluted with a retention time of 20 min (data not shown). This compound was also readily converted into C-26-deoxymonensin A by treatment with HF. It appears that C-26-deoxy-*epi*-monensin A is a poor substrate for MonE, the cytochrome P450 hydroxylase that is responsible for hydroxylation of the terminal C-26 position [8, 9].

Nonenzymatic Cyclization to Form Monensins

If MonBI and MonBII have been correctly identified as the enzymes that control the conversion of a triepoxide intermediate, probably protein-bound, into a polyether, then in their absence such intermediates should accumulate. The products seen in fermentation extracts of *monB* mutants ought then to reflect a balance between the chemical degradation of such species, their chemical or enzymatic release if they are protein bound, and the specificity of the C-3-O-methyltransferase and C-26-hydroxylase enzymes that are present as part of the monensin biosynthetic pathway. The observation that C-3-O-demethylmonensins A and B are the major products from all *monB* mutant strains shows, first, that epoxide ring opening and formation of the polyether rings with the correct regio- and stereospecificity is a chemically favored process under these conditions. Second, it shows that O-methylation at C-3 occurs either before polyether ring formation or before release of the monensin product from a protein, or both. Further, it seems that in the absence of methylation at C-3-OH, nucleophilic attack by the C-5 hydroxyl group on the C-9 carbonyl takes place preferentially to form the *natural* epimer of the spiroketal. This nonenzymatic kinetic control means that the subsequent cyclization gives C-3-O-demethylmonensins with the correct configuration (Figure 4).

Once the A ring has formed (Figure 4), the resulting hemiacetal hydroxyl opens the first epoxide to form the B ring, by nucleophilic attack at the more hindered carbon and with inversion at this center. This chemical preference can be rationalized on the basis that the alternative attack at the less hindered carbon would be a kinetically disfavored *6-endo-tet* cyclization in violation of Baldwin's rules [26]. Also, inversion at the tertiary center can be understood if acid catalysis promotes significant opening of the epoxide in the transition state, allowing the developing carbocation to be captured by the incoming hydroxyl nucleophile. This "loose S_N2" mechanism avoids the sterically disfavored S_N2 mechanism, while ensuring stereochemical inversion. Such a mechanism has been exploited in the construction of synthetic cyclic polyethers [27, 28]. It is also the basis of the mechanism proposed for limonene epoxide hydrolase [16] (Figure 3C). The same principles would apply to subsequent closure of the C ring of monensin (Figure 4). Formation of the D ring also involves a favorable *exo-tet* S_N2 ring closure, and the final reversible hemiacetal ring closure would be expected to give the natural configuration as the thermodynamically favored product.

The isolation of *epi*-monensins A and B and of C-26-deoxy-*epi*-monensins A and B as minor products from strains mutant in either or both of the *monB* genes
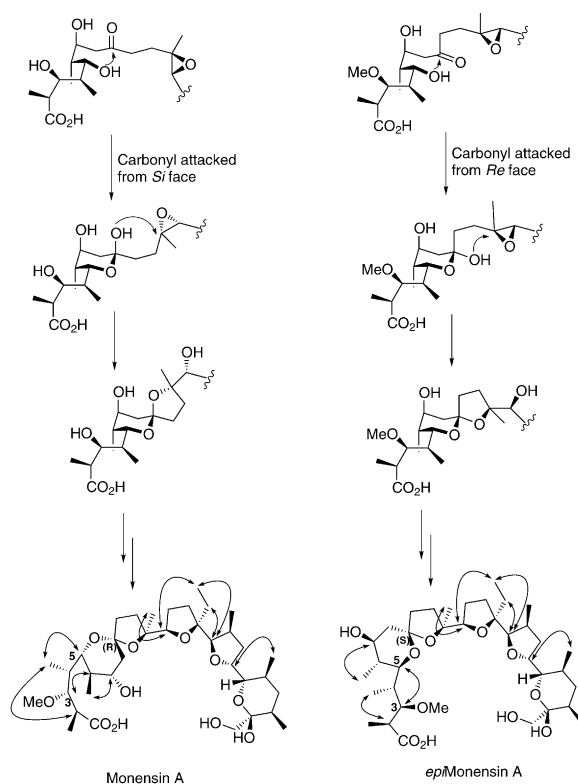

Figure 4. Modes of A Ring Closure Leading to Monensin A and C-9-*epi*-Monensin

The unnatural epimer results from nucleophilic attack at the opposite face of the C-9-carbonyl group to form the A ring hemiacetal. This alternative configuration is trapped as the spiroketal as the B ring is closed. [1]H-NOESY correlations are indicated by double-headed arrows. Protons are omitted for clarity.

reveals a second alternative (minor) fate for putative triepoxide intermediates, in the absence of MonB proteins. If the C3-hydroxy is methylated in the tri-epoxide intermediate, the unnatural spiroketal epimer appears to be kinetically favored, leading to the *epi*-isomer.

Cyclization Intermediates from MonB-Deficient Strains Are Chemically Competent for Conversion into Monensins

The nature of the faster-eluting, more polar metabolites noted earlier as minor components in the LC-MS analysis of the *monB* mutants is crucial for our proposal that the MonB enzymes govern polyether ring formation from the putative triepoxide. These species have molecular ions coincident with those of monensin A (693.5), monensin B and demethylmonensin A (679.5), and demethylmonensin B (665.5), but they are present in quantities too small to allow direct structural determination as yet. We reasoned that if these minor components represented species at the correct oxidation state but incompletely cyclized (Figure 5), then their cyclization should be accelerated by acid catalysis. The minor components were purified by HPLC, pooled, and treated with HF. Complete conversion of the material with molecular ion 679.5 to authentic C-3-O-demethyl monensin A and monensin B was observed (Figure 6). Similarly, the components with molecular ion 693.5 shifted to coelute
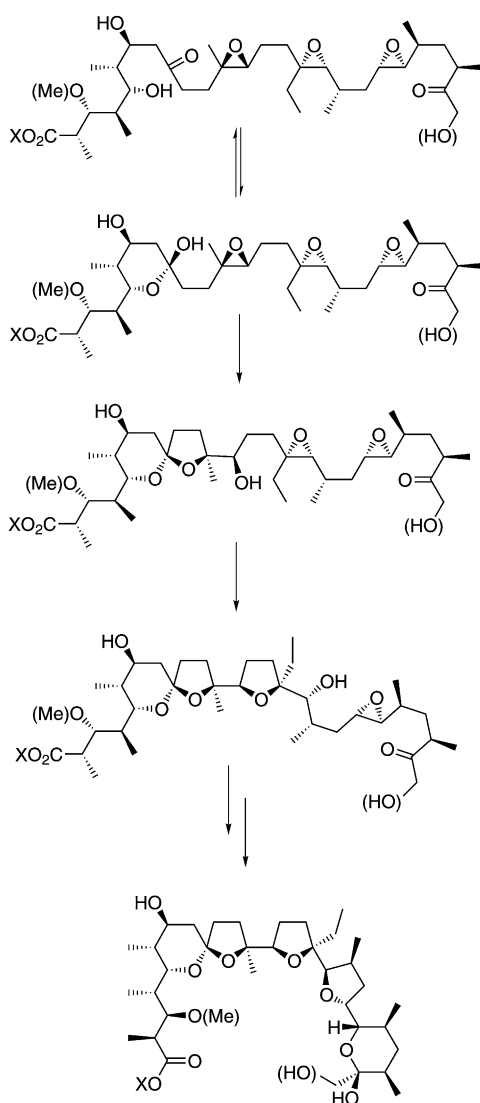
Figure 5. Proposed Intermediates in the Nonenzymatic Cyclization of a Triepoxide Metabolite Obtained When Monensin Biosynthesis Is Blocked by Mutation in One or More *monB* Genes
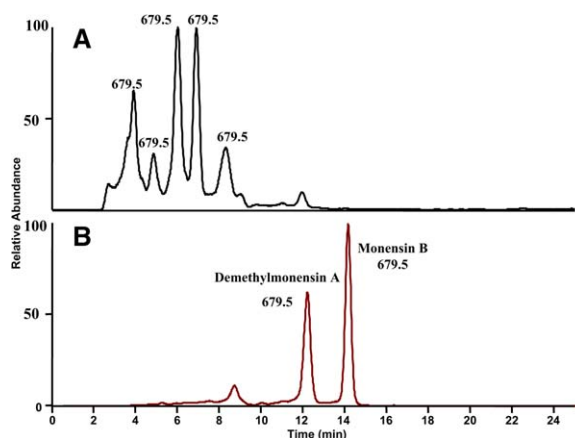

Figure 6. Acid-Catalyzed Cyclization of Putative Intermediate Species in Monensin Biosynthesis

Cyclization intermediates having the same mass as monensin B and demethylmonensin A (*m/z*, 679.5), but eluting earlier during chromatography, were separated by LC-MS. Upon treatment with HF, these intermediates cyclized to both demethylmonensin A (ca. 12 min) and monensin B (ca. 14 min). The vertical scales of the LC-MS traces are not identical.

MonB-Type Enzymes as Epoxide Hydrolases Involved in Polyether Ring Formation

The product of the gene *monCII*, previously proposed as governing epoxide ring opening in monensin biosynthesis, shows significant sequence and structural similarity, over about 260 amino acids, to the epoxide hydrolases of the α,β hydrolase family [30]. However, closer examination has revealed that the active site nucleophile in MonCII would be a serine residue rather than the conserved aspartate residue of this family; thus, the normal acyl intermediate would be replaced in MonCII by a much more stable ether intermediate. Also, few of these epoxidases are known to hydrolyze trisubstituted epoxides, in contrast to the limonene epoxide hydrolase [18]. As will be discussed elsewhere [13], we have reassigned MonCII as a thioesterase required for release of protein bound intermediates in monensin biosynthesis.

Since neither MonBI nor MonBII can support monensin biosynthesis on its own, the respective roles of MonBI and MonBII in catalyzing the successive formation of the polyether rings in monensin remain to be determined. The pattern of products in MonBI- and MonBII-deficient mutants appears to be identical, which argues that their actions are somehow coordinated. The protein NanI, involved in nanchangmycin biosynthesis, carries homologs of MonBI and MonBII in, respectively, its N-terminal and C-terminal halves [10] (Figure 2A). Further homology modeling (data not shown) suggests that MonBI and MonBII could, in principle, exist as a heterodimer in *S. cinnamonensis*. Whatever the protein arrangement turns out to be, from the present results it is clear that each ring closure in polyether formation occurs stepwise in a definite order, under enzymatic control of one or more MonB-type enzymes.

This model can be extended to the biosynthesis of much more complex polyethers, such as brevetoxin. As has been previously pointed out [31], if the stepwise or cascade opening of a polyepoxide is invoked [32] to explain the biosynthesis of this marine toxin, it must

with authentic monensin A, and those with molecular ion 665.5 shifted to coelute with authentic C-3-O-demethyl monensin B (data not shown). These results give strong support to the identification of the MonB enzymes as epoxide hydrolases involved in polyether ring formation. It shows, first, that C-26-hydroxylation can occur before either methylation or polyether ring formation. Second, it shows that *monB* genes are clearly not required for the formation of intermediate species that appear to have the correct geometry and to be at the correct oxidation level to give rise to monensins by ring opening/cyclization. The presence of MonB enzymes apparently accelerates, but does not change, the stereochemical course of polyether ring formation, compared to the acid-catalyzed process. Control of the spiroketal center by the MonB proteins could be achieved if the relevant MonB epoxide hydrolase is highly specific [29] and accepts only one epimer of the A ring hemiacetal.
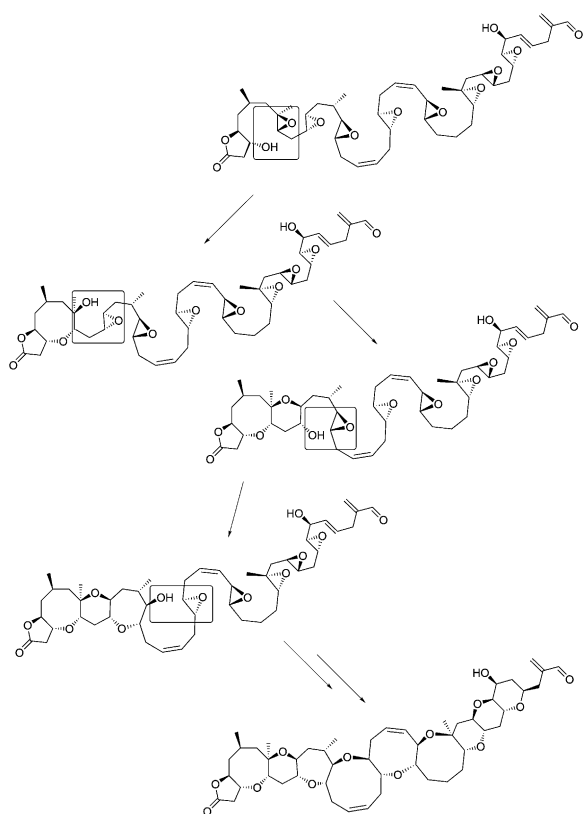
Figure 7. Proposed Stepwise Cyclization in the Biosynthesis of the Marine Toxin Brevetoxin, Catalyzed by a MonB-like Epoxide Hydrolase

The boxed regions in each intermediate indicate the loci for the successive action of an epoxide hydrolase.

involve a series of nine successive *endo-tet* cyclizations, each kinetically disfavored and in violation of Baldwin's rules. It is thus highly unlikely that a spontaneous, non-enzymatic cascade of epoxide openings is occurring here. A stepwise mechanism, as proposed for monensin cyclization, is much more attractive (see Figure 7). Successive closure of each ring by a highly specific epoxide hydrolase would present the substrate for the next epoxide hydrolase. In this case, each substrate is stereochemically identical, so only one MonB-like enzyme might be required to carry out all nine cyclizations.

Significance

Monensin is one of the most studied polyether antibiotics and is from one of the largest classes of bioactive polyketide natural products. Biosynthesis of polyethers involves polyketide chain formation on a modular polyketide synthase and a remarkable process of oxidative cyclization. Monensin biosynthesis has been proposed to involve a triepoxide intermediate that undergoes regiospecific and stereospecific ring opening and concomitant polyether ring formation, but the enzymology has remained obscure. We show here, from analysis of the polyketide products of mutations in the *monB* genes of the monensin biosynthetic gene cluster, together with homology modeling of the

MonB enzymes by using the recently determined structure of limonene epoxide hydrolase as a structural template, that the MonB enzymes, previously tentatively assigned as isomerases involved in altering the configuration of the initially formed polyketide, are the key epoxide hydrolase/cyclase enzymes in monensin biosynthesis. Based on this analysis, MonB-like enzymes may also be involved in the formation of the spectacular ladder polyether structures of marine toxins such as brevetoxin. These insights open the way to a complete deconvolution of the enzymology of polyether biosynthesis and will facilitate the engineering of polyether biosynthetic pathways to produce altered bioactive products.

Experimental Procedures

Culture Conditions
Seed cultures of wild-type and monensin-overproducing strains of *Streptomyces cinnamonensis* and *monB*-deficient mutants of these strains were grown in tryptic soy broth medium in flasks fitted with springs at 30°C and 200 rpm for 24 hr. These cultures (2.5 ml) were then used to inoculate 25 ml of either a proprietary germinative medium (I. Agayn, personal communication) or SM16-1 medium [9] in a 250 ml Erlenmeyer flask and were grown at 32°C and 200 rpm for 24–48 hr. From these seed cultures, each 2.5 ml portion was used to inoculate 40 ml of either an oil-based monensin production medium or SM16-1 in a 250 ml Erlenmeyer flask. The cultures were grown at 32°C and 200 rpm for 12 days. The relative humidity was maintained at 90%. Flasks were weighed before the start of fermentation, and any loss by evaporation was compensated for with sterile water.

Extraction and Purification of *epi*-Monensin A
The combined culture broth (1 liter) was centrifuged at 7500 rpm for 45 min, the supernatant was extracted three times with ethyl acetate (800 ml), and the combined organic fractions were evaporated in vacuo. The residue was redissolved in hexane and shaken vigorously with an equal volume of methanol:water (75:25 v/v). This mixture was then centrifuged at 7500 × g for 30 min, and the methanolic layer was removed. This was repeated twice with fresh methanol:water. The combined methanolic fractions were evaporated in vacuo and then lyophilized. The oily extract was dissolved in minimal ethyl acetate and passed twice through a silica column (35 × 100 mm), eluting with ethyl acetate:methanol (95:5). The solvent was removed in vacuo, and the residue was redissolved in minimal ethyl acetate and loaded onto a silica column (35 × 110 mm) packed in ethyl acetate (containing 5% methanol v/v):dichloromethane (2:1 v/v) and eluted with the same solvent mixture. Fractions were analyzed by LC-MS, and those containing the desired product were combined and evaporated in vacuo. This sample was then further purified through silica by using the same method as in the previous step. The relevant fractions (from LC-MS analysis) were pooled, and the solvent was removed. The sample was then redissolved in methanol (1.5 ml) and purified by preparative HPLC by using a Phenomenex Luna 10 μm C18(2) reverse-phase column (2120 × 250 mm). The solvent gradient used was from 80% methanol, 20% aqueous ammonium acetate (20 mM) to 100% methanol over 30 min, at a flow rate of 15 ml min⁻¹. Fractions were collected at 30 s intervals and analyzed by LC-MS. The fractions containing pure *epi*-monensin A were combined and evaporated as much as possible in vacuo and lyophilized. The product was then desalted by using an Isolute C18(EC) 500 mg cartridge (Jones Chromatography Ltd., Pontypridd, UK), and the product was lyophilized to yield C-9-*epi*-monensin A (~250 μg) as a white powder. Other metabolites were purified in the same manner.

Epimerization of *epi*-Monensin A
A sample of *epi*-monensin A (~5–10 μg) was dissolved in acetonitrile (1 ml). One drop of 48% aqueous hydrofluoric acid was added, and the reaction mixture was stirred at room temperature for 2 hr. The reaction mixture was adjusted to ~pH 9 with aqueous sodium

hydroxide (1 M), and the acetonitrile was removed in vacuo. The aqueous residue was extracted twice with ethyl acetate (1.5 ml), the organic extracts were combined and dried over anhydrous $MgSO_4$, and the solvent was removed. The sample was dissolved in HPLC-grade methanol (200 μl) and analyzed by LC-MS.

Cyclization of Intermediates Obtained from Cultures of *S. cinnamonensis monB* Mutants

Shake cultures were grown in SM16-1 medium [9] from a tryptic soy broth inoculum for 5 days at 30° and 200 rpm. The culture broth supernatant (50 ml) was extracted twice with ethyl acetate (50 ml), and the combined fractions were dried and then evaporated in vacuo. The crude product was adsorbed to a plug of silica and eluted with ethyl acetate, and the dried product was redissolved in methanol. The extract was analyzed by LC-MS, and the early-eluting metabolites were collected separately. These were dried, redissolved in acetonitrile, and treated with hydrofluoric acid, as described for the epimerization of *epi*-monensin A.

Mass Spectrometric Analysis of *epi*-Monensin A

Accurate mass analyses were performed on a BioApex II (4.7 Tesla) Fourier-transform cyclotron resonance instrument (Bruker Daltonics, Billerica, MA). Solutions were infused from the Analytica ESI source at 100 μl min^{-1}. CID fragmentation was performed on the isolated ions with CO_2 as the collision gas.

Expression and Purification of MonBI from Recombinant *Escherichia coli*

The *monBI* gene was amplified by PCR by using cosmid S23 encoding part of the monensin gene cluster as template [20] and oligonucleotide primers 5′-monB3-NdeI (5′-CGCATATGAACGAGTTCGCCC GCAAG-3′) and 3′-MonB3-NotI (5′-TAGCGGCCGCGCCGAGGACC GTGAGAT-3′), which introduced, respectively, an NdeI site at the 5′ end and a NotI site at the 3′ end. The purified fragment was cloned in pUC18, excised as a NdeI-NotI fragment, and ligated into expression plasmid pET-20b(+) (Novagen), which had been cut with the same enzymes. This gave plasmid pMonB3-20, encoding MonBI with a C-terminal hexahistidine tag, housed in *E. coli* strain BL21-CodonPlus (DE3)-RP (Stratagene). A single colony of this recombinant strain was used to inoculate 10 ml LB medium supplemented with glucose (1 g/liter), 50 μg/liter carbenicillin, and 34 μg/liter chloramphenicol, and the culture was grown overnight at 30ºC, then used as an inoculum for 1 liter LB medium supplemented as described above. When the absorbance at 600 nm reached 0.8, IPTG was added to 0.5 mM concentration, and induction was allowed to proceed for 3 hr. Cells were harvested by centrifugation at 5000 × g for 20 min at 4ºC to yield approximately 3 g wet weight of cells. The cells were suspended in 600 mM potassium phosphate buffer (pH 7.5), containing 400 mM NaCl, 5 mM imidazole, and 1 mM phenylmethanesulphonyl fluoride, and disrupted by two successive passages through a French pressure cell operated at 1000 psi. Cell debris was removed by centrifugation, the cleared lysate was incubated with 1 ml Ni-NTA resin (Qiagen), and the mixture was gently agitated on a rotary shaker at 4ºC for 1 hr. The resin was packed into a column, and, after washing with the same buffer, MonBI was eluted by a linear gradient of increasing imidazole concentration (up to 250 mM imidazole) in the same buffer, in 40 fractions each of 5 ml, at 1 ml/min. The fractions containing essentially pure MonBI were desalted on a small HiPrep column (Pharmacia Biotech), concentrated by using a spin concentrator (molecular weight Cut off of 5000 Da) (Millipore), and stored frozen at −80ºC.

Small-Angle X-Ray Scattering Analysis of MonBI Protein

Data were collected at Station 2.1, Synchrotron Radiation Source, Daresbury Laboratory by using a 2D multiwire proportional counter at sample-to-detector distances of 1.25 and 4.25 m. Data from matching buffers (50 mM Tris-HCl buffer [pH 7.0] and 100 mM NaCl) were collected and subtracted from the protein profiles. MonB1 solutions at concentrations ranging from 4 to 10 mg/ml and pH 4–8 were analyzed at 20ºC. The radius of gyration, R_g; the maximum particle dimension, D_{max}; and the intraparticle distance distribution function, ($p[r]$), were calculated from the scattering data by using the indirect Fourier transform method program Gnom [33]. Molecular shapes were reconstructed from the scatter-

ing profile (after merging high- and low-resolution data) by using the ab initio procedure of simulating annealing with clustered spheres representing amino acid residues (Gasbor versions 1.8 and 2.0) [34]. Shape reconstruction results in a 3D arrangement of scattering centers (spheres 3.5 Å in diameter) that reproduce the 1D scattering curve in accordance with the experimental data. These are displayed by using the space fill option to produce the overall molecular shape.

Similarity Search and Protein Modeling

The sequence of MonBI was compared with all protein sequences deposited in SWISS-PROT by using the Blast v2.0 program [35]. A PSI-BLAST search produced an alignment between MonBI and homologous proteins that highlights conserved residues in the epoxide hydrolase family. Homologous proteins with known structure were identified by using the FUGUE [14] homology recognition server. FUGUE searches for homologs in the structural profile library derived from the structure-based alignments in the HOMSTRAD database [36] and, using the environment-specific substitution tables, automatically generates the best alignments for the top hits. The alignment produced by FUGUE for the highest-scoring hit was formatted with JOY [37] and was analyzed visually to highlight the conservation of structurally and functionally important residues. The model of MonBI was constructed with MODELLER [38]. A final energy and structure minimization was done by using the SYBYL (Tripos, Inc., St. Louis, MO) force field. The model was validated with PROCHECK [39], VERIFY3D [40], JOY, and by visual inspection with 3D graphics software. Computer renderings of structures were created by using the program PyMOL [41].

Supplemental Data

Supplemental Data including LC-MS, NMR data for *epi*-monensin, details of protein expression and purification, and SAXs data for MonBI are available at http://www.chembiol.com/cgi/content/full/13/4/453/DC1/.

References

1. Westley, J.W. (1981). Polyethers. In Antibiotics IV Biosynthesis, J.W. Corcoran, ed. (New York: Springer-Verlag Publishers), pp. 41–73.
2. Shimizu, Y., Chou, H.N., Bando, H., Van Duyne, G., and Clardy, J. (1986). Structure of brevetoxin A (GB-1 toxin), the most potent toxin in the Florida red tide organism *Gymnodinium breve* (*Ptychodiscus brevis*). J. Am. Chem. Soc. *108*, 514–515.
3. Yasumoto, T., and Murata, M. (1993). Marine toxins. Chem. Rev. *93*, 1897–1909.
4. Riddell, F.G. (1992). Ionophoric antibiotics. Chem. Br. *28*, 533–537.
5. Westley, J.W., Evans, R.H., Harvey, G., Pitcher, R.G., and Pruess, D.L. (1974). Biosynthesis of lasalocid I. Incorporation of ^{13}C and ^{14}C labelled substrates into lasalocid A. J. Antibiot. (Tokyo) *27*, 288–297.
6. Cane, D.E., Liang, T.-C., and Hasler, H. (1981). Polyether biosynthesis. Origin of the oxygen atoms of monensin A. J. Am. Chem. Soc. *103*, 5962–5965.

7. Townsend, C.A., and Basak, A. (1991). Experiments and speculations on the role of oxidative cyclization chemistry in natural product biosynthesis. Tetrahedron *47*, 2591–2602.

8. Leadlay, P.F., Staunton, J., Oliynyk, M., Bisang, C., Cortés, J., Frost, E., Hughes-Thomas, Z.A., Jones, M.A., Kendrew, S.G., Lester, J.B., et al. (2001). Engineering of complex polyketide biosynthesis—insights from sequencing of the monensin biosynthetic gene cluster. J. Ind. Microbiol. Biotechnol. *27*, 360–367.

9. Oliynyk, M., Stark, C.B.W., Bhatt, A., Jones, M.A., Hughes-Thomas, Z.A., Wilkinson, C., Oliynyk, Z., Demydchuk, Y., Staunton, J., and Leadlay, P.F. (2003). Analysis of the biosynthetic gene cluster for the polyether antibiotic monensin in *Streptomyces cinnamonensis* and evidence for the role of *monB* and *monC* genes in oxidative cyclisation. Mol. Microbiol. *49*, 1179–1190.

10. Sun, Y., Zhou, X., Dong, H., Tu, G., Wang, M., Wang, B., and Deng, Z. (2003). A complete gene cluster from *Streptomyces nanchangensis* NS3226 encoding biosynthesis of the polyether ionophore nanchangmycin. Chem. Biol. *10*, 431–441.

11. Cho, H., Choi, G., Choi, K.Y., and Byung-Ha, O. (1998). Crystal structure and enzyme mechanism of Δ^5-3-ketosteroid isomerase from *Pseudomonas testeroni*. Biochemistry *37*, 8325–8330.

12. Bhatt, A., Stark, C.B.W., Harvey, B.M., Gallimore, A.R., Spencer, J.B., Staunton, J., and Leadlay, P.F. (2005). Accumulation of an *E,E,E,*-triene by a polyether-producing polyketide synthase when oxidative cyclization is blocked. Angew. Chem. Int. Ed. Engl. *44*, 7075–7078.

13. Harvey, B.M., Jones, M.A., Hughes-Thomas, Z.A., Goss, R.M., Heathcote, M.L., Bolanos-Garcia, V.M., Kroutil, W., Staunton, J., Leadlay, P.F., and Spencer, J.B. (2005). Evidence that a novel thioesterase is responsible for polyketide chain release during biosynthesis of the polyether ionophore monensin. Chem. Biol-Chem., in press.

14. Shi, J., Blundell, T.L., and Mizuguchi, K. (2001). FUGUE: sequence-structure homology recognition using environment-specific substitution tables and structure-dependent gap penalties. J. Mol. Biol. *310*, 243–257.

15. Lundqvist, T., Rice, J., Hodge, C.N., Basarab, G.S., Pierce, J., and Lindqvist, Y. (1994). Crystal structure of scytalone dehydratase—a disease determinant of the rice pathogen *Magnaporthe grisea*. Structure *2*, 937–944.

16. Arand, M., Hallberg, B.M., Zou, J., Bergfors, T., Oesch, F., van der Werf, J., de Bont, J.A.M., Jones, T.A., and Mowbray, S.L. (2003). Structure of *Rhodococcus erythropolis* limonene-1,2-epoxide hydrolase reveals a novel active site. EMBO J. *22*, 2583–2592.

17. Sultana, A., Kallio, P., Jansson, A., Wang, J.S., Niemi, J., Mantsala, P., and Schneider, G. (2004). Structure of the polyketide cyclase SnoaL reveals a novel mechanism for enzymatic aldol condensation. EMBO J. *23*, 1911–1921.

18. Kim, S.W., Cha, S.-S., Cho, H.-S., Kim, J.-S., Ha, N.-C., Cho, M.-J., Joo, S., Kim, K.-K., Choi, K.Y., and Oh, B.H. (1997). High-resolution crystal structures of Δ^5-3-ketosteroid isomerase with and without a reaction intermediate analogue. Biochemistry *36*, 14030–14036.

19. Holm, L., and Sander, C. (1998). Touring protein fold space with Dali/FSSP. Nucleic Acids Res. *26*, 316–319.

20. Robinson, A., Wu, P.S.-C., Harrop, S.J., Schaeffer, P.M., Dosztanyi, Z., Gillings, M.R., Holmes, A.J., Nevalainen, K.M.H., Stokes, H.W., Otting, G., et al. (2005). Integron-associated mobile gene cassettes code for folded proteins: the structure of Bal32a, a new member of the adaptable $\alpha + \beta$ barrel family. J. Mol. Biol. *346*, 1229–1241.

21. Hölz, A., Nairn, A.C., and Kuriyan, J. (2003). Crystal structure of a tetradecameric assembly of the association domain of Ca^{2+}/calmodulin-dependent kinase II. Mol. Cell *11*, 1241–1251.

22. Trewella, J. (1997). Insights into biomolecular function from small-angle scattering. Curr. Opin. Struct. Biol. *7*, 702–708.

23. Lopes, N.P., Stark, C.B.W., Hong, H., Gates, P.J., and Staunton, J. (2002). Fragmentation studies on monensin A and B by accurate mass electrospray tandem mass spectrometry. Rapid Commun. Mass. Spectrom. *16*, 414–420.

24. Perron, F., and Albizati, K.F. (1989). Chemistry of spiroketals. Chem. Rev. *89*, 1617–1661.

25. Ishihara, J., Sugimoto, T., and Murai, A. (1998). Studies on the stability of 1,7,9-trioxadispiro[5.1.5.2]pentadecane system: the common tricyclic moiety in pinnatoxins. Synlett *6*, 603–606.

26. Baldwin, J.E. (1976). Rules for ring closure. J. Chem. Soc. Chem. Comm. *11*, 734–736.

27. Hoye, T.R., and Suhadolnik, J.C. (1985). Symmetry-assisted synthesis of triepoxide stereoisomers of *E,Z,E,*-dodeca-2,6,10-trien-1,12-diol and their cascade reactions to 2,5-linked bistetrahydrofurans. J. Am. Chem. Soc. *107*, 5312–5313.

28. Koert, U. (1995). Stereoselective synthesis of oligo-tetrahydrofurans. Synthesis (Mass.) *1995*, 115–132.

29. Arand, M., Cronin, A., Oesch, F., Mowbray, S.L., and Jones, T.A. (2003). The tell-tale structures of epoxide hydrolases. Drug Metab. Rev. *35*, 365–383.

30. Jong, R.M., and Dijkstra, B.W. (2003). Structure and mechanism of bacterial dehalogenases: different ways to cleave a carbon-halogen bond. Curr. Opin. Struct. Biol. *13*, 722–730.

31. Rein, K.S., and Borrone, J. (1999). Polyketides from dinoflagellates: origins, pharmacology and biosynthesis. Comp. Biochem. Physiol. B Biochem. Mol. Biol. *124*, 117–131.

32. Lee, M.S., Qin, G., Nakanishi, K., and Zagorski, M.G. (1989). Biosynthetic studies of brevetoxins, potent neurotoxins produced by the dinoflagellate *Gymnodinium breve*. J. Am. Chem. Soc. *111*, 6234–6241.

33. Semenyuk, A.V., and Svergun, D.I. (1991). *GNOM* - a program package for small-angle scattering data processing. J. Appl. Crystallogr. *24*, 537–540.

34. Svergun, D.I., Petoukhov, M.V., and Koch, M.H.J. (2001). Determination of domain structure of proteins from X-ray solution scattering. Biophys. J. *80*, 2946–2953.

35. Altschul, S.F., Madden, T.L., Schaeffer, A.A., Zhang, J., Zhang, Z., Miller, W., and Lipman, D.J. (1997). Gapped BLAST and PSI-BLAST: a new generation of protein database search programs. Nucleic Acids Res. *25*, 3389–3402.

36. De Bakker, P.I.W., Bateman, A., Burke, D.F., Miguel, R.N., Mizuguchi, K., Shi, J., and Blundell, T.L. (2001). HOMSTRAD: adding sequence information to structure-based alignments of homologous protein families. Bioinformatics *17*, 748–749.

37. Mizuguchi, K., Deane, C.M., Blundell, T.L., Johnson, M.S., and Overington, J.P. (1998). JOY: protein sequence-structure representation and analysis. Bioinformatics *14*, 617–623.

38. Sali, A., and Blundell, T.L. (1993). Comparative protein modelling by satisfaction of spatial restraints. J. Mol. Biol. *234*, 779–815.

39. Laskowski, R.A., MacArthur, M.W., Moss, D.S., and Thornton, J.M. (1993). PROCHECK: a program to check the stereochemical quality of protein structures. J. Appl. Crystallogr. *26*, 283–291.

40. Luthy, R., Bowie, J.U., and Eisenberg, D. (1992). Assessment of protein models with three-dimensional profiles. Nature *356*, 83–85.

41. DeLano, W.L. (2002). The PyMOL User's Manual (San Carlos, CA: DeLano Scientific).